# Spatial heterogeneity of sedimentary organic carbon in fjords around Stavanger, Norway – implications for upscaling

Markus Diesing[1], Reidulv Bøe[1], Sigrid Elvenes[1], Jochen Knies[1,2], Craig Smeaton[3]

[1]Geological Survey of Norway, Trondheim, Norway
[2]iC3: Centre for ice, Cryosphere, Carbon and Climate, Department of Geosciences, UiT The Arctic University of Norway, Tromsø, Norway
[3]School of Geography and Sustainable Development, University of St Andrews, St Andrews, United Kingdom

*Correspondence to*: Markus Diesing (markus.diesing@ngu.no)

**Abstract.** Fjords are steep sided glacially carved troughs that have been inundated by the sea. Several global assessments have aimed to establish the role of fjords in the carbon cycle. According to these studies, fjords bury 18 Tg of organic carbon per year, and 55% to 62% of that organic carbon is terrestrially sourced. Such quantitative estimates, while important for understanding the role of fjords in the global carbon cycle, often rest on data compilations that might not be representative for fjord environments as a whole due to unaccounted spatial heterogeneity in terms of substrate types, depositional environments and characteristics of sedimentary organic carbon. Here, we present a local case study from fjords around Stavanger (Norway). Based on detailed investigations, we show that the seabed is heterogeneous in terms of substrate types covering the full grain-size spectrum from mud to boulders. Seabed areas where fine-grained sediment, and hence organic carbon, accumulates account for 50% of the area while the remainder is characterised by coarse-grained sediment indicating erosion and transport. In depositional areas, rates of organic carbon accumulation vary between 18.7 g $m^{-2}$ $yr^{-1}$ and 82.6 g $m^{-2}$ $yr^{-1}$ and stocks from 0.1 kg $m^{-2}$ and 1.37 kg $m^{-2}$. The fraction of labile organic matter varies between 19% and 44%, while $\delta^{13}C$-values of the organic carbon fraction range from -27.44‰ to -21.23‰, indicating a strong variability of the sources of organic carbon over a comparatively small area. Taken together, these results attest to high environmental variability and spatial heterogeneity in the study site, putting several assumptions used in global assessments into question. We suggest steps to achieve more realistic results when upscaling from local studies to a higher level. Using available data on organic carbon accumulation rates from Norwegian coastal areas, we demonstrate how local results could be upscaled in a more robust way. We arrive at a tentative estimate of 0.41 – 3.68 Tg $yr^{-1}$ of organic carbon accumulating in surface sediments (upper 10 cm) of fjords in mainland Norway.

## 1 Introduction

Fjords (also known as fiords, lochs and loughs) are over-deepened, mid to high-latitude estuaries which have been, or are presently being, excavated or modified by land-based ice (Howe et al., 2010; Syvitski et al., 1987). Globally, fjords cover an area of 445,859 $km^2$ according to Dürr et al. (2011) or 258,899 $km^2$ following a more recent estimate by Laruelle et al.

(2024). Despite their limited surface area on the order of 0.1% of the global ocean, it has been estimated that they bury between 17 and 20 Tg $yr^{-1}$ of organic carbon, equivalent to 11% of the annual marine organic carbon burial globally (Smith et al., 2015). These high rates have been attributed to very high area-normalised burial rates, about one hundred times as large as the global ocean average (Smith et al., 2015). A reanalysis by Cui et al. (2016), yielded a wider range of 6.1 to 31 Tg $yr^{-1}$ of organic carbon burial. Between 55 and 62% of the organic carbon buried in fjords globally and 76% in northwest Europe is terrestrially derived (Cui et al., 2016). The burial of marine and terrestrial organic carbon in global fjords may hence provide an important climate regulation service.

Smith et al. (2015) acknowledged in their supplementary information that the burial rates might be biased towards high values because the sediment cores in their global dataset tended to be located in depositional zones or fjord basins with higher sediment accumulation rates to obtain higher age resolution. However, they believed that this bias was small, based on results from one fjord in Norway, which showed predominantly depositional zones. Conversely, a recent study showed that fjords in Scotland and Ireland are heterogeneous in terms of substrate type and organic carbon content (Smeaton and Austin, 2019), leading to lower organic carbon burial estimates than otherwise expected (Smeaton et al., 2021).

The total mass of organic carbon that is buried annually in a defined area (OCB) can be calculated by multiplying organic carbon content (G), mass accumulation rates (MAR), the burial efficiency (BE) and the area under consideration (A):

$$OCB = G \cdot MAR \cdot BE \cdot A \quad (1)$$

G, MAR and BE can be obtained from a dated sediment core; however, an estimate of OCB would strictly speaking be only applicable to the coring site of size $A = \pi \cdot r^2$, where r is the radius of the coring tube. To what extent the results from an individual coring site are applicable to a larger area will depend on the spatial heterogeneity of the seabed. Upscaling of site-specific organic carbon burial rates to a larger area would therefore require an understanding of that spatial heterogeneity, which in turn could inform a sampling design for obtaining a representative sample of organic carbon burial rates.

Smeaton and Austin (2019) showed that mid-latitude fjords in Scotland and Ireland are highly heterogeneous both in sediment type and organic carbon content and concluded that further understanding of this spatial heterogeneity provides a foundation to reevaluate global organic carbon burial rates in fjords. While these authors focussed on sediment heterogeneity and how this relates to organic carbon content, here we go a step further by mapping substrate type, depositional environment, organic carbon accumulation rates, stocks, reactivity and provenance. Overall, the objectives of this study are twofold: (1) to characterise the spatial heterogeneity of organic carbon stored in surficial (0 – 10 cm sediment depth) fjord sediments and (2) to estimate organic carbon accumulation within our study site located north of the city of Stavanger, southwest Norway. Based on our data, we illustrate that global studies which estimate organic carbon burial in fjords (Cui et al., 2016; Smith et al., 2015) might indeed be biased towards high values. Finally, we propose a framework for more realistic upscaling from individual core data to higher levels (e.g., site, region or global).

## 2 Materials and methods

### 2.1 Study site

Our research is focussed on the marine area of Stavanger municipality in southwest Norway (Figure 1). The study area is within Boknafjorden, which is one of the larger fjords in Norway. Boknafjorden is wide and open in the outer and middle parts, with a number of larger and smaller islands. It has an outer threshold in the west and several inner fjord arms with local names, some with local thresholds. Several of the fjord areas between islands also have local fjord names. The length of the fjord from the outer threshold to the innermost fjord arm is 96 km, while the total surface area is 1579 $km^2$. The drainage area surrounding Boknafjorden is 7000-8000 $km^2$. Several rivers supply freshwater to the fjord, especially during snow melting in spring to early summer and during heavy rainfall. The wider study site was mapped as part of the project Marine Base Maps for the Coastal Zone (https://www.ngu.no/geologisk-kartlegging/marine-grunnkart-kystnaer-havbunnskartlegging, last access: 15/12/2025) and has an area of approximately 500 $km^2$, with water depths ranging between 0 m and 714 m. Seabed substrate type and sedimentary environment were mapped within this area. Nested within the wider study site lies the core study site with an approximate area of 250 $km^2$ and water depths between 0 m and 583 m below sea level. Investigations on organic carbon in surface sediments were restricted to this area, with generally oxygenated bottom waters.

### 2.2 Mapping of substrate type and sedimentary environment

Maps of seabed substrate types (sediment grain size) and sedimentary environment are two of the main products of the Marine Base Map pilot project in Stavanger, and they are both full-coverage, scale 1:20,000 vector maps. Thematic vector maps are created through expert interpretation of multibeam echosounder (MBES) bathymetry and backscatter data indicating the seabed's topography and relative hardness. Interpretation is guided by ground-truthing sediment samples and visual observations of the seabed from towed camera or a remotely operated vehicle (ROV), and aided by 2D acoustic sub-bottom profiling lines, LIDAR and aerial photography data from adjacent land areas, and any relevant legacy data from previous surveys. Further details on seabed mapping through expert interpretation can be found in Elvenes et al. (2019) and Bøe et al. (2022).

In the pilot project, we planned locations for video observations using a stratified random sampling design. Close to 300 video lines were recorded in the 500 $km^2$ study area during fieldwork in 2020. 80 grab sample stations were placed by the field geologist in soft-sediment areas where ground-truthing was needed, and an additional 10 multi corer stations for geochemical analyses were distributed in basins across the study area (Knies et al., 2021a).

Out of the Geological Survey of Norway's (NGU) 35 pre-defined classes of sediments used in seabed mapping (NGU, 2019a), we included 19 in the sediment grain size map of the wider study area. Most of these classes are also represented in the core study area of this project. In the map of sedimentary environment, we aim to describe whether conditions on the seabed allow for erosion or deposition of sandy or finer sediment. Five of NGU's standardised classes (NGU, 2019b) were

found in Stavanger, all of which are also represented in the core study area. The Marine Base Maps for the Coastal Zone pilot project conducted in 2020 - 2022 was the first of NGU's coastal mapping projects to include sedimentary environment.

### 2.3 Sampling design

We used a stratified random sampling design to avoid human bias and to facilitate modelling and spatial prediction based on 40 bulk samples of the uppermost 10 cm of the seabed sediment. Sampling within the core study site was limited to seabed areas where deposition from suspension, including limited local erosion of fine-grained sediments, was expected based on the mapped sedimentary environment (section 3.1). Of the 16 substrate classes found in these areas, six (human-made structures; gravel, cobbles and boulders; gravelly sand; sand; cobbles and boulders and cobbles/boulders covered by mud/sand) were excluded as they were deemed difficult to sample. However, these classes accounted for less than 1 $km^2$ of the seabed. Furthermore, the bathymetry data were classified into three depth intervals (shallow from 0 to 181 m, intermediate from 181 to 391 m, and deep from 391 to 583 m) using Jenk's natural breaks in ArcGIS 10.8.2. Strata were derived by combining the ten substrate classes with the three depth classes. Of the theoretically possible 30 strata, 24 did exist in the core study site. Before stations were randomly placed, we removed areas that were not accessible to sampling (aquaculture and military areas). Strata with an area of less than 1 $km^2$ were combined with suitable neighbouring strata. The stratified random placement of the stations was executed with the NOAA Sampling Design Tool for ArcGIS. The chosen allocation method was proportional, i.e., the number of stations per stratum was based on the relative area size of the strata. This led to 38 out of 40 stations being automatically allocated by the sampling tool. The two remaining stations were allocated to two strata, which had not automatically received a station.

Of the 15 stations that fell into areas mapped as deposition from suspension, ten were randomly selected to collect short cores that were dedicated to dating and the calculation of accumulation rates (Figure 2).

### 2.4 Field sampling and laboratory analysis

Fieldwork was conducted from 13th to 17th June 2023 onboard the 24 m research vessel 'Geologen'. Short sediment cores and grab samples were collected at the planned stations. The choice of sampling equipment depended on the substrate type at each station. Homogeneous, fine-grained sediments (mud and sandy mud) were sampled with a multi corer, which was equipped with four tubes of 60 cm length with a diameter of 6.3 cm. The tubes are closed at the top and bottom as the sample is taken, so that each core sample is collected with an undisturbed sediment surface. In coarser substrate types with a higher proportion of sand and gravel content, the samples were taken with a van Veen grab. Bulk samples of the upper 10 cm of sediment were taken at each station. When the multi corer was used, the upper 10 cm were cut off with a plastic spatula and frozen in plastic bags. When using a grab, four 10 cm long samples were taken with a syringe, collected in a plastic bag and frozen. At ten of the 40 stations, samples were also taken for dating (Figure 2). A sediment core from the multi corer was cut into 2 cm slices down to 20 cm sediment depth. The slices were packed separately in plastic bags and frozen after weighing.

After fieldwork, all samples were sent to the laboratory at the NGU. The samples were freeze-dried and further analysed. Dry bulk density ($\rho_d$) was calculated from the total water content of a sample using an empirical equation (Flemming and Delafontaine, 2000). Total organic carbon content (G) was measured using a LECO SC632 sulphur/carbon analyser after acidification with diluted hydrochloric acid to remove inorganic carbon.

Station-wise organic carbon stocks (OCS) were calculated using measurements on dry bulk density ($\rho_d$) and total organic carbon content (G) and the sediment thickness (d = 0.1 m):

$$OCS\ (kg\ m^2) = \frac{G\ (\%)}{100\%} \cdot 1000 \cdot \rho_d (g\ cm^{-3}) \cdot d(m) \quad (2)$$

The carbon reactivity index (CRI) is a measure to characterise the thermal reactivity of organic matter (Smeaton and Austin, 2022a). The CRI represents a continuum of reactivity with a value of 0 indicating that the organic matter is fully reactive and a value of 1 indicating that the organic matter is not reactive. In reality, these extremes will not be reached. The CRI was determined based on thermogravimetric analysis at the University of St. Andrews, Scotland. Milled samples of approximately 20 mg were placed into 70 ml aluminium oxide crucibles before being placed into a Mettler Toledo TGA2 and heated from 40 °C to 1000 °C at a ramp heating rate of 10 °C $min^{-1}$ under a constant stream of $N_2$. Analytical accuracy of the TGA analysis was determined through the measurement of, calcium oxalate monohydrate using the same instrument parameters as the samples. Calcium oxalate monohydrate degrades at three distinct temperatures 150 °C, 500 °C and 750 °C (Hourlier, 2019). The calcium oxalate monohydrate (*n = 5*) thermograms on average deviate from the known thermal profile by 0.16 ± 0.04 °C and differences in mass loss between all standards by 1.23% ± 0.41%. The thermograms produced from these analyses were adjusted to a common temperature scale and clipped to the range 200 °C–650 °C to remove interference from absorbed water and non-organic material. The thermograms were normalised to the mass loss, to assure all thermograms were comparably scaled. Note that a high CRI value indicates a low fraction of labile organic matter and vice versa.

Stable carbon isotope analysis of the organic carbon fraction ($\delta^{13}C_{org}$) was undertaken at the University of St Andrews. Approximately 12 mg of milled sediment was placed into silver capsules. The samples then underwent acid fumigation (Harris et al., 2001) to remove carbonate ($CaCO_3$), post fumigation the samples were dried for 48 hr at 40°C and sealed prior to analysis. Stable isotope analysis was undertaken using an elemental analyser coupled to an isotope ratio mass spectrometer. Quality control was assured by repeat analysis of high organic carbon sediment standard (B2151) with reference values for C of 7.45% ± 0.14% and $\delta^{13}C$ of −28.85 ± 0.10‰. The reference standards (*n = 10*) deviated from their known values by: OC = 0.05%, $\delta^{13}C$ = 0.09‰. The isotope values are reported in standard delta notation relative to Vienna Peedee belemnite (VPDB).

Samples for dating were sent to the Gamma Dating Center Copenhagen at the University of Copenhagen, where the activity of the isotopes $^{210}Pb$, $^{226}Ra$ and $^{137}Cs$ was analysed using gamma spectrometry. The measurements were carried out on a

Canberra ultralow-background Ge-detector. $^{210}$Pb was measured via its gamma-peak at 46.5 keV, $^{226}$Ra via the granddaughter $^{214}$Pb (peaks at 295 and 352 keV) and $^{137}$Cs via its peak at 661 keV. Constant rate of supply modelling has been applied on the profile using a modified method (Andersen, 2017; Appleby, 2001), where the activity below the lower-most sample is calculated based on a regression of unsupported $^{210}$Pb vs accumulated dry density. Based on the radiometric data, the age of the sediment at different depths and ultimately mass accumulation rates (MAR) could be determined for each analysed core sample. In addition to the ten cores collected in 2023, we also included data from two cores collected and analysed as part of the Marine Base Maps for the Coastal Zone project (Knies et al., 2021a). These were collected with the same type of multi corer (Figure 6).

Organic carbon accumulation rates ($OCAR_{10}$) were calculated from average mass accumulation rates ($\overline{MAR}$) and organic carbon content ($\bar{G}$) of the upper 10 cm of the analysed cores:

$$OCAR_{10}\ (g\ m^{-2}\ yr^{-1}) = 1000 \cdot \overline{MAR}(kg\ m^{-2} yr^{-1}) \cdot \frac{\bar{G}(\%)}{100\%} \quad (3)$$

### 2.5 Modelling and spatial prediction

We use a data-driven machine learning approach to model and spatially predict the response variables organic carbon stock, carbon reactivity index and stable carbon isotopes based on a set of environmental predictor variables. Since this approach belongs to the class of empirical models, it does not inform about cause and effect or underlying mechanisms, but.is rather optimised for reality and precision (Guisan and Zimmermann, 2000). The response variables were spatially predicted based on models derived from the 40 bulk samples. The number of stations (n = 12) was, however, not sufficient to model and spatially predict organic carbon accumulation rates.

Raster grids of predictor variables were initially selected based on availability and potential relevance. The same predictor variables were used for all three response variables. These included acoustic data from multibeam surveys (bathymetry and backscatter strength), the Euclidean distance to the nearest shoreline, semi-quantitative substrate composition (mud, sand, gravel, cobbles/boulders and bedrock) derived from the mapped substrates, photosynthetically active radiation (400 – 700 nm wavelength) reaching the seabed, modelled salinity, temperature and current velocity at the seabed (mean, standard deviation, minimum and maximum) and the 90$^{th}$ percentile of the wave orbital velocity at the seabed (Table S1). Note that the final set of predictor variables was determined algorithmically by optimising a performance criterion (see below) and varied between the three models.

Modelling was carried out with Quantile Regression Forests (Meinshausen, 2006). Since the response data were collected as a probability sample (stratified random sample in this case), it was sufficient to estimate model performance with 10-fold cross validation without the need to account for spatial autocorrelation in the data (Meyer and Pebesma, 2022; Wadoux et al., 2021). The model performance was assessed with three metrics: the mean error (which measures bias), the root mean

squared error (which measures accuracy) and the r-squared (which measures the explained variance). The set of predictor variables finally selected for prediction was determined through forward feature selection (Meyer et al., 2018) by optimising the root mean squared error. The algorithm first trains models based on all possible combinations of two predictor variables. The best performing combination is retained and tested for the best performance with a third variable. Additional variables are added until the performance stops improving.

Based on the selected models, we spatially predicted the response variables and their area of applicability (Meyer and Pebesma, 2021). We also estimated the area of applicability (Meyer and Pebesma, 2021). Within the area of applicability, the combination of predictor variables is similar to what the model has been trained with. Outside the area of applicability, the predictions might extrapolate beyond the predictor variable space that has been captured by the model and results might thus be unreliable. We quantified spatially explicit model uncertainty with the 90% prediction interval, PI90 (Heuvelink, 2014). The PI90 gives the range of values within which the true value is expected to occur nine times out of ten, with a one in 20 probability for each of the two tails (Arrouays et al., 2014). It is defined as

$$PI90 = q_{0.95} - q_{0.05} \quad (4)$$

with $q_{0.95}$ and $q_{0.05}$ being the 0.95 and 0.05 quantiles of the distribution, respectively.

Finally, we corrected the predicted organic carbon stocks for the fraction of coarse substrates. We assumed that cobbles, boulders and bedrock do not contain organic carbon. The predicted stocks ($OCS_{pred}$) were hence corrected ($OCS_{corr}$) based on the coarse fraction (CSF) according to:

$$OCS_{corr} = OCS_{pred} \cdot (1 - CSF) \quad (5)$$

The reservoir size and its uncertainty were calculated by summing corrected organic carbon stocks and associated uncertainties over all pixels of the resulting raster layers and multiplying with the area of one pixel (2,500 $m^2$).

### 2.6 Regionalisation

An unsupervised classification was carried out to provide a regionalisation of the study site. The regionalisation was based on the spatially predicted variables organic carbon stocks, carbon reactivity index and stable carbon isotopes. A k-means clustering was conducted utilising the algorithm of Hartigan and Wong (1979). Prior to clustering, the input variables were centred by subtracting the mean of the raster layer from each pixel value and normalised by dividing the pixel value by the standard deviation of the raster layer|. The selection of the number of clusters to be requested was aided by an elbow plot. Box plots of the clusters for the three variables were created based on a subsample (n = 10,000) to visualise the properties of the clusters.

### 2.7 National scale estimates

To put our results from the local study in a wider context, we analysed maps of seabed substrate and sedimentary environment from other coastal areas derived by the Geological Survey of Norway over the last 20 years or so. Initially, these GIS vector maps were clipped to the area covered by the Norwegian fjord catalogue (https://data.norge.no/en/datasets/e34a3447-dc8b-4661-9361-ec72da8109af/fjordkatalogen). They were subsequently dissolved as multipart features by substrate type and sedimentary environment, respectively. Finally, the geodesic area was calculated with the Add Geometry Attributes tool. The analysis was performed in ArcGIS Desktop 10.8.2.

We also compiled data from other fjords in mainland Norway and calculated organic carbon accumulation rates for the upper 10 cm ($OCAR_{10}$) following eq. 3.

## 3 Results

### 3.1 Substrate type and depositional environment

Full-coverage, high-quality MBES data of 1 to 2 m resolution combined with a high number of seabed observations allowed for detailed mapping of substrate type in the study area (Figure 3). Backscatter data were especially useful in delineating areas of soft sediment (sandy or muddy substrate types reflecting less of the acoustic echosounder signal than what coarser seabed does), while bathymetry data revealed landforms like moraine ridges, talus cones or bedrock outcrops associated with harder substrates. In shallow areas the data could even show individual boulders. Keeping to a map scale of 1:20 000 requires some generalisation, as individual map elements cannot be too small to distinguish at the intended scale. Much of the Stavanger seabed is also of a heterogeneous nature, with both sand/mud and rocks/boulders present in the same area. This heterogeneity is expressed in map form by the use of mixed classes such as “Sand, gravel, cobbles and boulders” or “Mud and sand with gravel, cobbles and boulders”.

As shown in Table 1, around a third of the seabed in the study area is defined as “Thin or discontinuous sediment cover on bedrock”. Note that the classification does not distinguish between different types of sediment cover, and as such may include both fine-grained and very coarse material covering bedrock in various thicknesses. The seabed type is also found at all depths (Figure 3). Mud and sandy mud cover 12.0% and 13.6% of the seabed, respectively, dominating deeper areas and some isolated basins. Another 11.9% of the seabed is defined as the heterogeneous substrate type “Sand, gravel, cobbles and boulders”, found predominantly in areas shallower than 200 m. Other substrate types cover less than 10% of the seabed, with only “Gravelly sandy mud” and “Mud and sand with gravel, cobbles and boulders” exceeding 5%. 48.5 $km^2$ of the area are characterised by deposition from suspension, and 78.4 $km^2$ by deposition from suspension with local erosion of fine-grained sediments. The remainder (126.5 $km^2$) either shows signs of erosion or deposition of mainly sand from bottom currents. This means that half of the area is depositional in character (Figure 4).

At the national scale, the inshore areas covered by the fjord catalogue amount to 89,368.4 $km^2$. Of this, 13,768 $km^2$ (15.4%) have so far been mapped with regard to substrate types and 2,604.9 $km^2$ (2.9%) with regard to the sedimentary environment. Fine-grained sediments (mainly mud, sandy mud and muddy sand but including clay, organic mud, mud with sediment blocks, silt, sandy silt and silty sand (NGU, 2019a)) cover 33.1% of the mapped area. Environments conducive to sediment deposition (deposition from suspension and deposition from suspension, local erosion of fine-grained sediments) cover 35.5% of the mapped seabed.

### 3.2 Data exploration

The three response variables organic carbon stock, stable carbon isotope values and the carbon reactivity index are plotted in a generalised pairs plot together with the water depth at the sampling locations (Figure 5). Organic carbon stocks display a distribution with a dominant peak at approximately 0.75 kg $m^{-2}$. Stable carbon isotope values exhibit a bimodal distribution with peaks at approximately -22.5‰ and -26‰, indicating marine and terrestrial sources, respectively. The distribution of CRI values is also bimodal but has a dominant peak at 0.725 and a secondary peak at 0.625. All three response variables show strong and statistically significant ($p < 0.001$, $n = 40$) correlations with each other. Organic carbon stocks are negatively correlated with stable carbon isotope and CRI values, while the latter two exhibit a positive correlation. The response variables are also correlated with water depth, albeit less strongly.

### 3.3 Organic carbon accumulation rates

To obtain reliable results, sediment mixing due to bioturbation or other processes has to be negligible; otherwise, the accumulation rates will be overestimated. To minimise the risk of sediment mixing, sediment cores for dating were only collected from the area mapped as deposition from suspension. There were two cores with significant mixing (marked by ** in Figure 6) and two cores with possible mixing (marked by * in Figure 6), while the rest of the cores showed no signs of sediment mixing based on examination of the $^{210}Pb$ profiles. The calculated accumulation rates in the cores with sediment mixing are therefore probably overestimated. At the same time, the values are low compared to data from cores without mixing. To obtain a more representative overview of the accumulation rates, we therefore do not exclude the cores with signs of sediment mixing but note that these rates might be too high.

Estimated organic carbon accumulation rates varied from 18.7 g $m^{-2}$ $yr^{-1}$ to 82.6 g $m^{-2}$ $yr^{-1}$ (22 – 73 g C $m^{-2}$ $yr^{-1}$, when excluding the minimum and maximum values) (Figure 6), with a mean value of 44.6 g $m^{-2}$ $yr^{-1}$ and a median of 40.5 g C $m^{-2}$ $yr^{-1}$. There are no clear spatial patterns apparent and organic carbon accumulation rates can change over short distances, e.g. in Talgjefjorden between Rennesøy and Finnøy.

At the national level, $OCAR_{10}$ could be calculated for 28 cores from five regions. Apart from Stavanger (Diesing et al., 2024b; Knies et al., 2021a), these were Sunnhordland (Knies et al., 2024), Sunnmøre (Knies et al., 2021b), Sør-Troms (Lepland et al., 2012) and Troms (Knies et al., 2022). The data from Stavanger was supplemented with four values from

285 Høgsfjorden and Lysefjorden (Duffield et al., 2017), immediately to the east of our study site (Figure 1). The data are compiled in Table S2. The median $OCAR_{10}$ of these 28 records is 40.5 g C $m^{-2}$ $yr^{-1}$ (Table 2).

### 3.4 Organic carbon stocks

Seven predictor variables were selected for the final organic carbon stock model (gravel content, maximum bottom salinity, mean bottom temperature, maximum bottom current velocity, 90% percentile of the wave orbital velocity at the seabed,
290 mean bottom salinity and minimum bottom temperature). The model had a mean error (ME) of 0.012 kg $m^{-2}$, a root mean squared error (RMSE) of 0.174 kg $m^{-2}$, an explained variance ($R^2$) of 59.2% and an area of applicability equal to 98% of the total area.

The corrected organic carbon stocks varied between 0.1 kg $m^{-2}$ and 1.37 kg $m^{-2}$ (Figure 7), while the PI90 ranged from 0.14 kg $m^{-2}$ to 1.15 kg $m^{-2}$ (Figure S1). Organic carbon stocks were highest in the central part of Mastrafjorden between
295 Rennesøy and Mosterøy and some smaller areas in the eastern part of the study site. Stocks are lowest in scattered areas mapped as thin or discontinuous sediment cover on bedrock (Figure 3). In total, 83.2 ± 55.7 Gg of organic carbon are stored in the surface sediments of the mapped area.

### 3.5 Sources of organic carbon

Three predictor variables were selected for the final $\delta^{13}C$ model (bathymetry, maximum bottom current velocity and the 90%
300 percentile of the wave orbital velocity at the seabed). The model had an ME of 0.039‰, an RMSE of 0.822‰, an $R^2$ of 82.7% and an area of applicability (AOA) equal to 90% of the total area.

Predicted $\delta^{13}C$-values varied between -27.33‰ and -21.78‰ (Figure 8), while the PI90 ranged from 1.47‰ to 6.21‰ (Figure S2). The δ13C-values are highest in Boknafjorden in the west of the study site and in Talgjefjorden between Rennesøy and Finnøy.

305 **3.6 Reactivity of organic carbon**

Four predictor variables were selected for the final CRI model (fraction of the seafloor that is occupied by bedrock, standard deviation of bottom temperature, 90% percentile of the wave orbital velocity at the seabed and the maximum bottom current velocity). The model had an ME of 0.001, an RMSE of 0.027, an $R^2$ of 80.3% and an area of applicability equal to 87% of the total area.

310 Predicted CRI values varied between 0.59 and 0.78 (Figure 9), while the PI90 ranged from 0.04 to 0.21 (Figure S3). The spatial patterns resemble those of the stable carbon isotope values (Figure 8). This might be expected since $\delta^{13}C$ and CRI exhibit a strong positive correlation (Figure 5).

### 3.7 Regionalisation

Based on an elbow plot, a four-cluster solution was selected. The cluster numbers were ordered in a way that the mean $\delta^{13}C$-values per cluster decreased (Figure 10). Cluster 1 (dark blue) is characterised by intermediate organic carbon stocks, high $\delta^{13}C$-values and high CRI-values and is located in the central (deeper) parts of Boknafjorden, Talgjefjorden and Finnøyfjorden. Cluster 2 (light blue) exhibits low organic carbon stocks, a high variability in $\delta^{13}C$-values and relatively high CRI-values. The cluster has a high association with seabed areas dominated by a thin or discontinuous sediment cover on bedrock and other coarse substrates. Cluster 3 (light green) has intermediate organic carbon stocks, relatively low $\delta^{13}C$-values and intermediate to low CRI-values. The cluster is mainly found in Finnøyfjorden, Fognafjorden and Gardssundfjorden. Cluster 4 (dark green) shows the highest organic carbon stocks, the lowest $\delta^{13}C$-values and the lowest CRI-values. This cluster is most prominent in Mastrafjorden and restricted areas in the northeast of the study site.

## 4 Discussion

This study builds on previous work by Smeaton and Austin (2019) who have explored the spatial heterogeneity of sedimentary organic carbon in Scottish and Irish fjords. However, it differs from that study by mapping key metrics of sedimentary organic carbon relating to accumulation, storage, reactivity and provenance, rather than using substrate type as a proxy for organic carbon content.

### 4.1 Environmental variability

We provide evidence for strong variability along various environmental gradients (substrate type, depositional environment, organic carbon accumulation rates, stocks reactivity and source). Substrate types vary from mud (clay and silt) to cobbles and boulders, and a third of the seabed is bedrock covered by a thin and discontinuous layer of sediment. Fine-grained sediments (mud, sandy mud and muddy sand) collectively cover just over 30% of the seafloor in Stavanger, similar to the percentage at the national scale (33%). Comparable fractions are found to cover the seabed in the fjords of Scotland and Ireland (Smeaton and Austin, 2019). Half of the mapped area in Stavanger is characterised by transport and erosion, while deposition of fine-grained sediment is restricted to the other half. At the national scale, depositional areas account for 35% of the mapped seabed in mainland Norway.

Calculated organic carbon accumulation rates vary between 19 and 83 g C $m^{-2}$ $yr^{-1}$ in Stavanger. In the nearby fjords to the east of our study site, values of 13 – 171 g C $m^{-2}$ $yr^{-1}$ were reported for Høgsfjorden and Lysefjorden, with the highest rates recorded at the head of Lysefjorden closest to the Lyseåna river (Duffield et al., 2017). Comparable rates of 43 – 133 g C $m^{-2}$ $yr^{-1}$ were also found in Raunefjorden (Włodarska-Kowalczuk et al., 2019). The mean value of 44.6 g $m^{-2}$ $yr^{-1}$ for Stavanger falls within the range of mean values reported from fjord systems in northwest Europe: 28.0 g C $m^{-2}$ $yr^{-1}$ in east

Iceland (Watts et al., 2025), 38.0 g C $m^{-2}$ $yr^{-1}$ at the west coast of Sweden (Watts et al., 2024) and 57.1 g C $m^{-2}$ $yr^{-1}$ in Scotland (Smeaton et al., 2021).

Corrected organic carbon stocks range from 0.1 to 1.37 kg $m^{-2}$ in Stavanger, indicating considerable variability. However, the variability is lower than in fjords of Scotland and Ireland, where especially muddy sediments have stocks of 3 kg $m^{-2}$ and more (Smeaton and Austin, 2019). Presumably, this difference in variability is linked to the different size of the areas. It might be assumed that on a national scale the variability in stock sizes in Norway is larger than in Stavanger.

Measured CRI values vary between 0.56 and 0.81 (i.e., labile organic matter fraction of 19% – 44%) in Stavanger. This falls within the range of values of 0.45 – 0.9 in inshore (fjords and estuaries) surface sediments outside hypoxic upper fjord basins in Scotland (Smeaton and Austin, 2022a). Organic matter sampled in these hypoxic basins has an even higher labile fraction of up to 69% (Smeaton and Austin, 2022a).

Measured $\delta^{13}C$-values range from -27.44‰ to -21.23‰, with a bimodal distribution showing peaks at -26‰ and -22.5‰ (Figure 5). The minima and maxima are close to reported terrestrial and marine end members in Norway and Scotland of -26.1‰ to -28.6‰ and -18.7‰ to -20.6‰, respectively (Faust and Knies, 2019; Knies and Martinez, 2009; Smeaton et al., 2021; Smeaton and Austin, 2017; Winkelmann and Knies, 2005). Using a two-endmember mixing model (Thornton and McManus, 1994) and assuming that the terrestrial (-28.56‰) and marine (-18.99‰) end member values determined by Smeaton and Austin (2022b) are applicable to our study site, indicates that the terrestrial fraction of organic carbon might range between 23% and 88%. These results demonstrate a strong variability of the sources of organic carbon over a comparatively small area. A high variability of sources was also found in fjords of the Swedish west coast (-27‰ to -20‰, Placitu et al., 2024) and in the fjords of Scotland (-29.7‰ to -19.5‰, Smeaton and Austin, 2022b), while in other regions $\delta^{13}C$-values are more constrained, e.g., Reyðarfjörður and Berufjörður in Iceland (-23.2‰ to -21.8‰, Watts et al., 2025) and Ofotfjorden, Tysfjorden and Vestfjorden in northern Norway (-23.8‰ to -20.9‰, Faust and Knies, 2019). Overall, these results indicate that the terrestrial fraction of organic carbon might deviate substantially from the average value of 76% for northwest Europe (Cui et al., 2016), echoing findings from Faust and Knies (2019).

In summary, we observe high variability especially regarding substrate types and the depositional environment, organic carbon accumulation rates and the source of organic carbon.

### 4.2 Spatial heterogeneity

Our results point towards strong spatial gradients in Stavanger. The central (deeper) parts of Boknafjorden, Talgjefjorden and Finnøyfjorden are characterised by high $\delta^{13}C$-values (cluster mean: -22.5‰) close to reported marine end member values of -18.7‰ to -20.6‰ in Norway and Scotland (Faust and Knies, 2019; Knies and Martinez, 2009; Smeaton et al., 2021; Smeaton and Austin, 2017; Winkelmann and Knies, 2005) and CRI values (cluster mean: 0.73) typical of coastal and offshore zones in Scotland (Smeaton and Austin, 2022a) (Cluster 1 in Figure 10). Boknafjorden is directly connected to the northern North Sea and marine water can enter the fjords in Stavanger via Boknafjorden, Talgjefjorden and Finnøyfjorden as evidenced by our data.

Conversely, shallow fjords like Mastrafjorden and the shallow areas between Finnøyfjorden and Strandafjorden in the northeast of the core study site are characterised by low $\delta^{13}C$-values (cluster mean: -26.1‰) close to terrestrial end member values of -26.1‰ to -28.6‰ (Faust and Knies, 2019; Knies and Martinez, 2009; Smeaton et al., 2021; Smeaton and Austin, 2017; Winkelmann and Knies, 2005) indicating strong terrestrial influence (Cluster 4 in Figure 10). CRI values (cluster mean: 0.62) are similar to those of inshore (fjords and estuaries) zones (Smeaton and Austin, 2022a). Marine influence is likely dictated by bathymetry. Remarkably, the strikingly different Clusters 1 and 4 are found in close proximity to each other, e.g. the distance between Talgjefjorden and Mastrafjorden is approximately 5 km. The two clusters are spatially separated by the two transitional Clusters 2 and 3.

Overall, we observe a strong positive correlation ($r = 0.845$, $p < 0.001$, $n = 40$) between provenance ($\delta^{13}C$) and reactivity (CRI) (Figure 5), which is also reflected in the spatial patterns of $\delta^{13}C$ and CRI (compare Figure 8 with Figure 9). We observe a gradient from marine-dominated, less labile organic carbon in deep water, especially in Boknafjorden (Cluster 1) to terrestrially-dominated, more labile organic carbon in shallow, narrow fjords and sheltered archipelagos in close proximity to land (Figure 10). This gradient pattern might indicate both high marine inflow and freshwater runoff according to the model of Faust and Knies (2019).

### 4.3 Upscaling of organic carbon accumulation rates to the site level

Organic carbon accumulation rates can vary over short distances (a few kilometres), as exemplified by three cores taken in Talgjefjorden (Figure 6). These cores encapsulate the full variability of calculated organic carbon accumulation rates (19 and 83 g C $m^{-2}$ $yr^{-1}$) in Stavanger. Presumably, the highest of the three rates is due to the coring location close to the centre of the basin, while the other two cores exhibiting lower rates have marginal positions in the basin. As the central coring location was deliberately chosen for the purpose of investigating the historical development of contamination (Knies et al., 2021a) while the other two locations were chosen randomly as described in section 2.3, these observed differences also highlight the influence of the sampling design. Using non-randomly selected coring locations will most likely bias the data towards high organic carbon accumulation rates.

In addition to the two cores from Knies et al. (2021a), we collected ten cores for dating from areas characterised by deposition from suspension (Figure 2). These 12 cores have a median organic carbon accumulation rate of 40.5 g C $m^{-2}$ $yr^{-1}$, while the size of the area where deposition from suspension occurs is 48.5 $km^2$. Assuming that the median organic carbon accumulation rate is representative of that area yields an organic carbon accumulation of 1,964 t C $yr^{-1}$. This figure is, however, an underestimation of the total mass of organic carbon accumulating within the study site, since it does not include areas characterised by deposition from suspension with local erosion of fine-grained sediments (Figure 2), which account for 78.4 $km^2$ of the seabed. Applying the median organic carbon accumulation rate to both zones with a total area of 126.9 $km^2$ yields an organic carbon accumulation of 5,139 t C $yr^{-1}$. However, this estimate is most likely too high, since the median organic carbon accumulation rate in the zone of deposition from suspension with local erosion of fine-grained sediments is

expected to be lower than that of the zone of deposition from suspension. The 'true' value therefore is expected to lie between 1,964 and 5,139 t C $yr^{-1}$.

Our data also serve as an illustration of how organic carbon accumulation (and hence burial) is likely overestimated in global studies (Cui et al., 2016; Smith et al., 2015). These studies make two implicit assumptions (Smeaton and Austin, 2019): (1) The seabed within fjords is homogeneous with regard to the depositional environment. (2) The estimated organic carbon burial rates contained in the global dataset are representative for the fjords they were obtained from. In this scenario, the area would be that of the study site (253.4 $km^2$) and the organic carbon accumulation rate might be based on the two cores from the contamination study of Knies et al. (2021a), in which coring sites were deliberately selected to favour high sediment accumulation rates for higher age resolution and to minimise sediment mixing through bioturbation and other processes. Under such circumstances, the median organic carbon accumulation rate is 77.7 g C $m^{-2}$ $yr^{-1}$ and the total organic carbon accumulation within the study site amounts to 19,689 t C $yr^{-1}$. This value is roughly four to ten times higher than our estimates above. While this factor of four to ten will not be universally applicable, our site-specific comparison illustrates that organic carbon accumulation rates in global studies are likely overestimated. In addition, the global fjord area is currently poorly constrained, with the estimate by Laruelle et al. (2024) being 58% of the estimate by Dürr et al. (2011), which has been used in global studies (Cui et al., 2016; Smith et al., 2015).

### 4.4 Requirements for realistic upscaling

We propose the following steps to achieve more realistic results when upscaling from individual core data to a higher level, be it local, regional, national, continental or global. These considerations apply to variables that relate to the surface area of the seabed, i.e. organic carbon accumulation rates and stocks.

Step 1. Derive a realistic estimate of the total fjord area. This should be relatively straight forward at the local to regional level. However, the higher the level becomes the more difficult it is to derive realistic estimates. Currently, the global fjord area is poorly constrained and there are no spatial products available. Higher level fjord maps might be derived through a GIS analysis utilising suitable data such as coastlines, bathymetry etc. Alternatively, fjord maps might be derived from remote sensing data analysed with machine learning algorithms similar to tidal flats (Murray et al., 2019).

Step 2. Estimate the fraction of seabed where fine-grained sediment accumulates. In Norway, these areas are mapped by experts as described in section 2.2. However, this process is time-consuming and requires suitable datasets (multibeam bathymetry, backscatter strength, sub-bottom, and ground-truthing data) to be collected in the first instance. As a proxy, sediment accumulation basins could be derived from existing seabed sediment maps by reclassifying mud-rich seabed types (Elvenes et al., 2019). However, these are likely to underestimate the true area where deposition of fine-grained sediments occurs. Alternatively, numerical models simulating sediment dynamics should be capable of identifying erosional and depositional areas. Due to the computational requirements of such models, they likely perform best on a local to regional level. Another option might be employing terrain variables derived from bathymetric data of sufficient resolution. Terrain variables such as roughness and bathymetric position index might be indicative of areas where sediment accumulates.

Step 3. Draw a representative sample of organic carbon accumulation rates or stocks. Ideally, a probability sample (such as a random or stratified random sample) should be drawn from the area for which an analysis is performed. However, such an approach is most likely restricted to local studies, as it involves the collection of a sufficient amount of new data. At higher levels, there is a need to include existing data from previous studies, but these data might be biased as discussed above. Note that in the case of organic carbon stocks, the sediments in erosional and non-depositional areas (typically sands and gravels) will to some extent contain organic carbon (Smeaton and Austin, 2019).

Step 4. Account for uncertainty. Rather than just providing an estimate based on mean values, we suggest considering the variability of the data. This could be achieved by providing low and high estimates based on certain percentiles of the data distribution, e.g., P5 and P95 (Diesing et al., 2017; Donato et al., 2011).

To demonstrate the above, we use data from mainland Norway to give a tentative estimate of annual organic carbon accumulation in Norwegian fjord sediments. We also discuss the current limitations and suggest improvements.

The total area of the Norwegian fjord catalogue amounts to $A_f$ = 89,368.4 km$^2$. The fraction of the seabed where deposition of fine-grained sediment dominates ($f_{dep}$) might be estimated to 25% (low), 33% (intermediate) and 50% (high estimate), based on the results from this study and Smeaton and Austin (2019). We use the data in Table 2 for values of organic carbon accumulation rates. In particular, we use the P5 for the low, the median for the intermediate and the P95 for the high estimate. We then calculate the annual organic carbon accumulation (OCA) for low, intermediate and high estimates by

$$OCA = A_f \cdot f_{dep} \cdot OCAR_{10}. \quad (6)$$

This yields 1.19 (0.41 – 3.68) Tg yr$^{-1}$ of organic carbon accumulating in surface sediments of fjords in mainland Norway. Given a lack of data on burial efficiencies and inconsistencies in their definition (Bradley et al., 2022), we refrain from calculating organic carbon burial.

There are currently several limitations to these estimates. The total area ($A_f$) covered by the fjord catalogue includes sea areas which would not qualify as fjords in a strict geomorphological sense. The seaward limit of the fjord catalogue is the baseline relative to which maritime zones are defined, rather than a sill that separates a fjord from the open sea. The actual fjord area of mainland Norway is hence lower. However, from a practical point of view the baseline is a suitable seaward boundary as it is also the landward limit for which organic carbon stocks and accumulation rates have been derived in offshore areas (Diesing et al., 2024a). Using the baseline as the seaward limit of coastal and inshore areas ensures that there is no gap between coastal and offshore mapping.

The fraction of seabed characterised by deposition of fine-grained sediments ($f_{dep}$) is based on 3% of the total area where the sedimentary environment has been mapped in Norway. This estimate is therefore currently tentative, and we use three different values to account for uncertainty in the estimate. Inshore and coastal mapping in Norway is, however, ongoing and the fraction of mapped seabed will increase over time, yielding improved estimates.

So far, we have collated data on organic carbon accumulation rates ($OCAR_{10}$) from five regions, 19 fjords and 28 coring stations. Again, the estimates are tentative and we use the 5$^{th}$ and 95$^{th}$ percentiles of the data distribution to account for uncertainty, similar to Donato et al. (2011) and Diesing et al. (2017). The true organic carbon accumulation rate is likely to lie between the low (0.41 Tg C yr$^{-1}$) and the high estimate (3.68 Tg C yr$^{-1}$). As for the fraction of seabed characterised by deposition of fine-grained sediments, it can be expected that more data will be collected over the coming years, and the estimates will improve.

It should also be noted that the 28 cores used for this analysis were all retrieved from areas characterised by deposition from suspension. Collecting dateable cores from areas that are dominated by deposition from suspension but also show local erosion of fine-grained sediments is a challenging task. This is highlighted by the fact that those four cores located close to the boundary between the two areas show signs of sediment mixing (Figure 6). Improved dating techniques might be necessary to obtain realistic organic carbon accumulation rates from such transitional sedimentary environments.

## 5 Conclusions

Based on detailed seabed mapping in fjords around Stavanger (Norway), we show that substrate types are highly variable and encompass the whole grain-size spectrum from mud to boulders. Areas where fine-grained sediments accumulate amount to 50% of the total mapped area. In these depositional areas, organic carbon accumulation rates and stocks vary considerably, as does the fraction of labile organic matter and the sources of organic carbon (marine vs terrestrial). This pronounced environmental variability, and spatial heterogeneity calls into question upscaling approaches that rely on implicit assumptions about the homogeneity of sediment type and depositional character and the representativeness of 'global' data compilations on organic carbon accumulation rates that are unlikely to hold. We conclude with suggestions of how upscaling from individual cores to higher levels could be improved.

## Code availability

All original code has been deposited at https://github.com/diesing-ngu/Stavanger_organic_carbon.

## Data availability

Input data to spatially predict organic carbon stocks, the carbon reactivity index and $\delta^{13}C$ have been deposited at https://zenodo.org/records/18172827 (Diesing and Smeaton, 2026)(Diesing and Smeaton, 2026).

## Supplement link

Supplement.docx

## Author contributions

Conceptualization, MD, RB; Data curation, MD; Funding acquisition, RB; Investigation, MD, SE, CS; Methodology, MD, RB; Project administration, RB, MD; Resources, RB; Software, MD; Validation, MD; Visualization; MD; Writing (original draft preparation), MD, SE, CS; Writing (review and editing), MD, RB, SE, JK, CS

## Competing interests

The authors declare that they have no conflict of interest.


## Acknowledgements

The authors would like to thank the captain and crew of R/V 'Geologen' for invaluable assistance during fieldwork.

## Financial support

This work was financially supported by Stavanger municipality.


## References


Andersen, T. J.: Some Practical Considerations Regarding the Application of 210Pb and 137Cs Dating to Estuarine Sediments, in: Applications of Paleoenvironmental Techniques in Estuarine Studies, edited by: Weckström Kaarina and Saunders, K. M. and G. P. A. and S. C. G., Springer Netherlands, Dordrecht, 121–140, https://doi.org/10.1007/978-94-024-0990-1_6, 2017.

Appleby, P. G.: Chronostratigraphic Techniques in Recent Sediments, in: Tracking Environmental Change Using Lake Sediments: Basin Analysis, Coring, and Chronological Techniques, edited by: Last William M. and Smol, J. P., Springer Netherlands, Dordrecht, 171–203, https://doi.org/10.1007/0-306-47669-X_9, 2001.

Arrouays, D., Grundy, M. G., Hartemink, A. E., Hempel, J. W., Heuvelink, G. B. M., Hong, S. Y., Lagacherie, P., Lelyk, G., McBratney, A. B., McKenzie, N. J., d.L. Mendonca-Santos, M., Minasny, B., Montanarella, L., Odeh, I. O. A., Sanchez, P. A., Thompson, J. A., and Zhang, G.-L.: Chapter Three - GlobalSoilMap: Toward a Fine-Resolution Global Grid of Soil Properties, vol. 125, edited by: Sparks, D. L., Academic Press, 93–134, https://doi.org/10.1016/B978-0-12-800137-0.00003-0, 2014.

Bøe, R., Bjarnadóttir, L. R., Elvenes, S., Dolan, M., Bellec, V., Thorsnes, T., Lepland, A., and Longva, O.: Revealing the secrets of Norway's seafloor - geological mapping within the MAREANO programme and in coastal areas, Geological Society, London, Special Publications, 505, 57–69, https://doi.org/10.1144/SP505-2019-82, 2022.

Bradley, J. A., Hülse, D., LaRowe, D. E., and Arndt, S.: Transfer efficiency of organic carbon in marine sediments, Nat. Commun., 13, 7297, https://doi.org/10.1038/s41467-022-35112-9, 2022.

Cui, X., Bianchi, T. S., Savage, C., and Smith, R. W.: Organic carbon burial in fjords: Terrestrial versus marine inputs, Earth Planet. Sci. Lett., 451, 41–50, https://doi.org/https://doi.org/10.1016/j.epsl.2016.07.003, 2016.

Diesing, M. and Smeaton, C.: Input data to spatially predict organic carbon stocks, carbon reactivity index and delta 13C in fjords around Stavanger, Norway, https://doi.org/10.5281/zenodo.18172827, January 2026.

Diesing, M., Kröger, S., Parker, R., Jenkins, C., Mason, C., and Weston, K.: Predicting the standing stock of organic carbon in surface sediments of the North–West European continental shelf, Biogeochemistry, 135, 183–200, https://doi.org/10.1007/s10533-017-0310-4, 2017.

Diesing, M., Paradis, S., Jensen, H., Thorsnes, T., Bjarnadóttir, L. R., and Knies, J.: Glacial troughs as centres of organic carbon accumulation on the Norwegian continental margin, Commun. Earth Environ., 5, 327, https://doi.org/10.1038/s43247-024-01502-8, 2024a.

Diesing, M., Knies, J., Elvenes, S., and Bøe, R.: Kartlegging av organisk karbon i sjøbunnssedimenter i Stavanger kommune, NGU-Rapport, 2024.015, 2024b.

Donato, D. C., Kauffman, J. B., Murdiyarso, D., Kurnianto, S., Stidham, M., and Kanninen, M.: Mangroves among the most carbon-rich forests in the tropics, Nature Geosci, 4, 293–297, 2011.

Duffield, C., Alve, E., Andersen, N., Andersen, T., Hess, S., and Strohmeier, T.: Spatial and temporal organic carbon burial along a fjord to coast transect: A case study from Western Norway, Holocene, 27, 1325–1339, https://doi.org/10.1177/0959683617690588, 2017.

Dürr, H. H., Laruelle, G. G., van Kempen, C. M., Slomp, C. P., Meybeck, M., and Middelkoop, H.: Worldwide Typology of Nearshore Coastal Systems: Defining the Estuarine Filter of River Inputs to the Oceans, Estuaries and Coasts, 34, 441–458, https://doi.org/10.1007/s12237-011-9381-y, 2011.

Elvenes, S., Bøe, R., Lepland, A., and Dolan, M.: Seabed sediments of Søre Sunnmøre, Norway, J. Maps, 15, 686–696, https://doi.org/10.1080/17445647.2019.1659865, 2019.

Faust, J. C. and Knies, J.: Organic Matter Sources in North Atlantic Fjord Sediments, Geochemistry, Geophysics, Geosystems, 20, 2872–2885, https://doi.org/10.1029/2019GC008382, 2019.

Flemming, B. W. and Delafontaine, M. T.: Mass physical properties of muddy intertidal sediments: some applications, misapplications and non-applications, Cont. Shelf Res., 20, 1179–1197, https://doi.org/10.1016/S0278-4343(00)00018-2, 2000.

Guisan, A. and Zimmermann, N. E.: Predictive habitat distribution models in ecology, Ecol. Modell., 135, 147–186, https://doi.org/10.1016/S0304-3800(00)00354-9, 2000.

Harris, D., Horwáth, W. R., and van Kessel, C.: Acid fumigation of soils to remove carbonates prior to total organic carbon or CARBON-13 isotopic analysis, Soil Science Society of America Journal, 65, 1853–1856, https://doi.org/https://doi.org/10.2136/sssaj2001.1853, 2001.

Hartigan, J. A. and Wong, M. A.: Algorithm AS 136: A K-Means Clustering Algorithm, J. R. Stat. Soc. Ser. C Appl. Stat., 28, 100–108, https://doi.org/10.2307/2346830, 1979.

Heuvelink, G. B. M.: Uncertainty quantification of GlobalSoilMap products, in: GlobalSoilMap: Basis of the global spatial soil information system, edited by: Arrouays, D., McKenzie, N., Hempel, J., Richer de Forges, A., and McBratney, A. B., CRC Press, Boca Raton, 335–340, 2014.

Hourlier, D.: Thermal decomposition of calcium oxalate: beyond appearances, J. Therm. Anal. Calorim., 136, 2221–2229, https://doi.org/10.1007/s10973-018-7888-1, 2019.

Howe, J. A., Austin, W. E. N., Forwick, M., Paetzel, M., Harland, R., and Cage, A. G.: Fjord systems and archives: a review, Geological Society, London, Special Publications, 344, 5–15, https://doi.org/10.1144/SP344.2, 2010.

Knies, J. and Martinez, P.: Organic matter sedimentation in the western Barents Sea region: Terrestrial and marine contribution based on isotopic composition and organic nitrogen content, Norwegian Journal of Geology, 89, 79–89, 2009.

Knies, J., Elvenes, S., and Bøe, R.: Sedimentasjonsmiljø og historisk utvikling i forurensingsstatus i sjøområdene i Stavanger kommune, NGU-Rapport, 2021.003, 84, 2021a.

Knies, J., Boitsov, S., Baeten, N. J., Elvenes, S., and Bøe, R.: Sedimentasjonsmiljø og historisk utvikling i forurensningsstatus i sjøområdene i kommunene Ålesund og Giske, NGU-Rapport, 2021.018, 67, 2021b.

Knies, J., Boitsov, S., Elvenes, S., and Bøe, R.: Sedimentasjonsmiljø og historisk utvikling i forurensningsstatus i sjøområde i kommunene Skjervøy, Kvænangen, og Nordreisa, NGU-Rapport, 2022.016, 64, 2022.

Knies, J., Boitsov, S., Elvenes, S., and Bøe, R.: Sedimentasjonsmiljø og historisk utvikling i forurensningsstatus i kommunene Sveio, Bømlo, Stord, Fitjar, Tysnes og Austevoll i Sunnhordland, NGU-Rapport, 2024.017, 67, 2024.

Laruelle, G. G., Rosentreter, J. A., and Regnier, P.: Extrapolation-Based Regionalized Re-evaluation of the Global Estuarine Surface Area, Estuaries and Coasts, 48, 34, https://doi.org/10.1007/s12237-024-01463-3, 2024.

Lepland, A., Jensen, H. K. B., Plassen, L., and Longva, O.: Forurensningsstatus i sjøbunnssedimenter i Astafjordområdet/Sør-Troms, NGU-Rapport, 2012.002, 37, 2012.

Meinshausen, N.: Quantile Regression Forests, Journal of Machine Learning Research, 7, 983–999, 2006.

Meyer, H. and Pebesma, E.: Predicting into unknown space? Estimating the area of applicability of spatial prediction models, Methods Ecol. Evol., 12, 1620–1633, https://doi.org/10.1111/2041-210X.13650, 2021.

Meyer, H. and Pebesma, E.: Machine learning-based global maps of ecological variables and the challenge of assessing them, Nat. Commun., 13, 2208, https://doi.org/10.1038/s41467-022-29838-9, 2022.

Meyer, H., Reudenbach, C., Hengl, T., Katurji, M., and Nauss, T.: Improving performance of spatio-temporal machine learning models using forward feature selection and target-oriented validation, Environmental Modelling & Software, 101, 1–9, https://doi.org/https://doi.org/10.1016/j.envsoft.2017.12.001, 2018.

Murray, N. J., Phinn, S. R., DeWitt, M., Ferrari, R., Johnston, R., Lyons, M. B., Clinton, N., Thau, D., and Fuller, R. A.: The global distribution and trajectory of tidal flats, Nature, 565, 222–225, https://doi.org/10.1038/s41586-018-0805-8, 2019.

NGU: Classification of Sediments Based on Grain Size Composition (Folk, 1954, Modified), 2019a.

NGU: Sedimentary Environment, 2019b.

Placitu, S., van de Velde, S. J., Hylén, A., Hall, P. O. J., Robertson, E. K., Eriksson, M., Leermakers, M., Mehta, N., and Bonneville, S.: Limited Organic Carbon Burial by the Rusty Carbon Sink in Swedish Fjord Sediments, J. Geophys. Res. Biogeosci., 129, e2024JG008277, https://doi.org/https://doi.org/10.1029/2024JG008277, 2024.

Smeaton, C. and Austin, W. E. N.: Sources, Sinks, and Subsidies: Terrestrial Carbon Storage in Mid-latitude Fjords, J. Geophys. Res. Biogeosci., 122, 2754–2768, https://doi.org/https://doi.org/10.1002/2017JG003952, 2017.

Smeaton, C. and Austin, W. E. N.: Where's the Carbon: Exploring the Spatial Heterogeneity of Sedimentary Carbon in Mid-Latitude Fjords, Front. Earth Sci. (Lausanne)., 7, 269, https://doi.org/10.3389/feart.2019.00269, 2019.

Smeaton, C. and Austin, W. E. N.: Quality Not Quantity: Prioritizing the Management of Sedimentary Organic Matter Across Continental Shelf Seas, Geophys. Res. Lett., 49, e2021GL097481, https://doi.org/10.1029/2021GL097481, 2022a.

Smeaton, C. and Austin, W. E. N.: Understanding the Role of Terrestrial and Marine Carbon in the Mid-Latitude Fjords of Scotland, Global Biogeochem. Cycles, 36, e2022GB007434, https://doi.org/https://doi.org/10.1029/2022GB007434, 2022b.

Smeaton, C., Yang, H., and Austin, W. E. N.: Carbon burial in the mid-latitude fjords of Scotland, Mar. Geol., 441, 106618, https://doi.org/https://doi.org/10.1016/j.margeo.2021.106618, 2021.

Smith, R. W., Bianchi, T. S., Allison, M., Savage, C., and Galy, V.: High rates of organic carbon burial in fjord sediments globally, Nat. Geosci., 8, 450–453, https://doi.org/10.1038/NGEO2421, 2015.

Syvitski, J. P. M., Burrell, D. C., and Skei, J. M.: Fjords and Their Study, in: Fjords: Processes and Products, edited by: Syvitski, J. P. M., Burrell, D. C., and Skei, J. M., Springer New York, New York, NY, 3–17, https://doi.org/10.1007/978-1-4612-4632-9_1, 1987.

Thornton, S. F. and McManus, J.: Application of Organic Carbon and Nitrogen Stable Isotope and C/N Ratios as Source Indicators of Organic Matter Provenance in Estuarine Systems: Evidence from the Tay Estuary, Scotland, Estuar. Coast. Shelf Sci., 38, 219–233, https://doi.org/https://doi.org/10.1006/ecss.1994.1015, 1994.

Wadoux, A. M. J.-C., Heuvelink, G. B. M., de Bruin, S., and Brus, D. J.: Spatial cross-validation is not the right way to evaluate map accuracy, Ecol. Modell., 457, 109692, https://doi.org/10.1016/j.ecolmodel.2021.109692, 2021.

Watts, E. G., Hylén, A., Hall, P. O. J., Eriksson, M., Robertson, E. K., Kenney, W. F., and Bianchi, T. S.: Burial of Organic Carbon in Swedish Fjord Sediments: Highlighting the Importance of Sediment Accumulation Rate in Relation to Fjord Redox Conditions, J. Geophys. Res. Biogeosci., 129, e2023JG007978, https://doi.org/https://doi.org/10.1029/2023JG007978, 2024.

Watts, E. G., Zautcke, K., Santos, I., Smeaton, C., Ljungberg, W., Cheung, H. L. S., Bonaglia, S., Politi, T., Liu, Z., and Bianchi, T. S.: Efficient Burial of Labile Organic Carbon in Sediments of Oxygenated Icelandic Fjords, Estuaries and Coasts, 48, 167, https://doi.org/10.1007/s12237-025-01582-5, 2025.

Winkelmann, D. and Knies, J.: Recent distribution and accumulation of organic carbon on the continental margin west off Spitsbergen, Geochemistry, Geophysics, Geosystems, 6, https://doi.org/https://doi.org/10.1029/2005GC000916, 2005.

Włodarska-Kowalczuk, M., Mazurkiewicz, M., Górska, B., Michel, L. N., Jankowska, E., and Zaborska, A.: Organic Carbon Origin, Benthic Faunal Consumption, and Burial in Sediments of Northern Atlantic and Arctic Fjords (60–81°N), J. Geophys. Res. Biogeosci., 124, 3737–3751, https://doi.org/https://doi.org/10.1029/2019JG005140, 2019.

630

**Table 1. Absolute and relative area occupied by substrate types**

| Substrate type | Area ($km^2$) | Area (% of total) |
|---|---|---|
| Mud | 30.37 | 12.0 |
| Sandy mud | 34.54 | 13.6 |
| Muddy sand | 11.72 | 4.6 |
| Sand | 6.85 | 2.7 |
| Gravelly sandy mud | 14.53 | 5.7 |
| Gravelly muddy sand | 5.31 | 2.1 |
| Gravelly sand | 8.52 | 3.4 |
| Sandy gravel | 1.12 | 0.4 |
| Sand, gravel, cobbles and boulders | 30.14 | 11.9 |
| Gravel and cobbles | 0.70 | 0.3 |
| Sand, gravel and cobbles | 10.10 | 4.0 |
| Gravel, cobbles and boulders | 2.34 | 0.9 |
| Cobbles and boulders | 0.07 | 0.0 |
| Mud and sand with gravel, cobbles and boulders | 12.62 | 5.0 |
| Mud/sand with cobbles/boulders | 0.01 | 0.0 |
| Cobbles/boulders covered by mud/sand | 0.07 | 0.0 |
| Thin or discontinuous sediment cover on bedrock | 84.02 | 33.2 |

**Table 2. Percentiles calculated for the 28 $OCAR_{10}$ values in g C $m^{-2}$ $yr^{-1}$ compiled in this study. P5 – 5th percentile; Q1 – 1st quartile; Q3 – 3rd quartile; P95 – 95th percentile.**

| 5% (P5) | 25% (Q1) | 50% (Median) | 75% (Q3) | 95% (P95) |
|---|---|---|---|---|
| 18.4 | 25.7 | 40.5 | 60.1 | 82.3 |

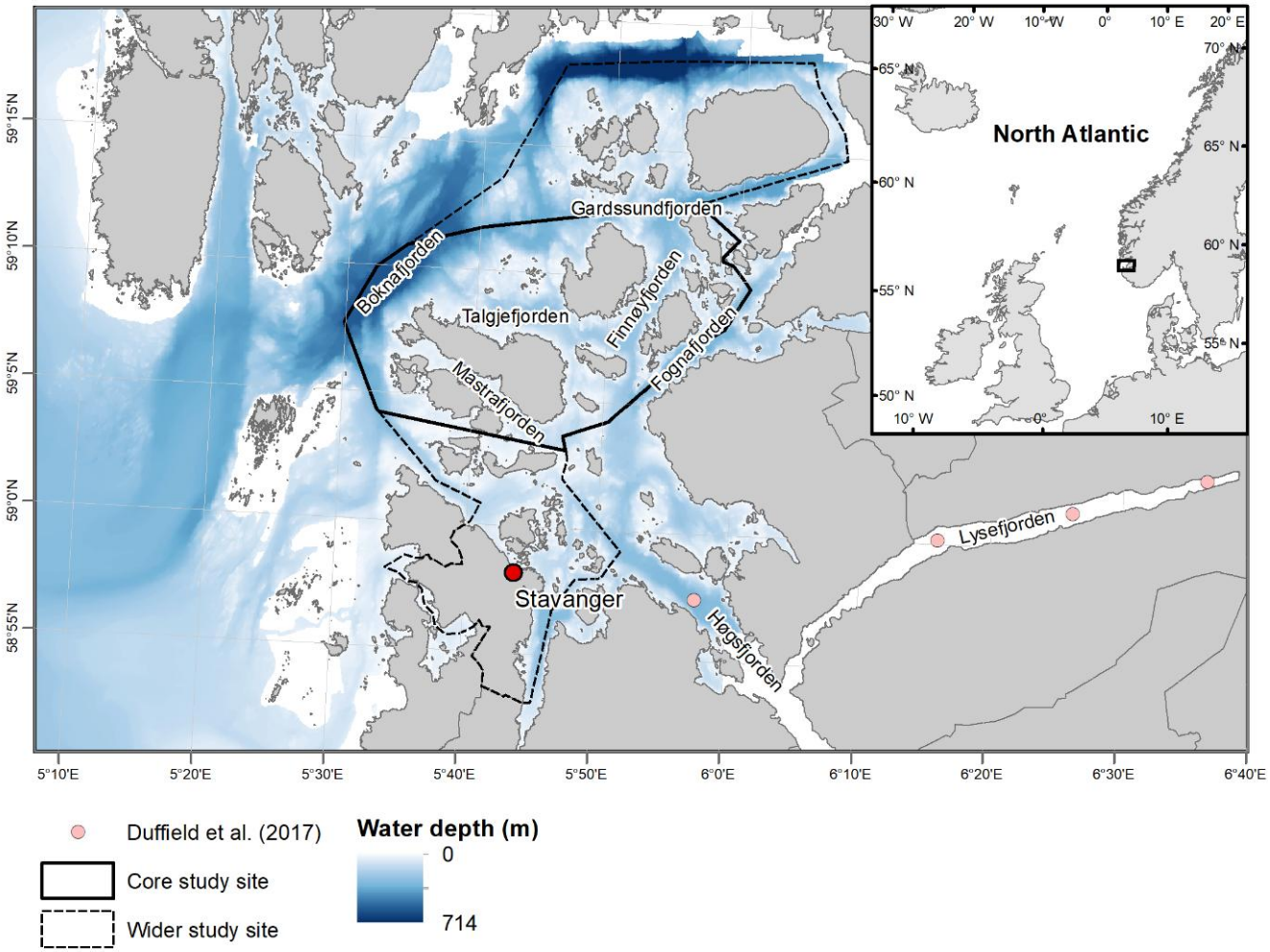


**Figure 1. Overview of the wider and core study sites. Also shown are coring locations from Duffield et al. (2017). Bathymetry data** 640 **available from Kartverket (hoydedata.no). White areas indicate no bathymetry data. The inset shows the location of the study site in northwest Europe (black rectangle).**

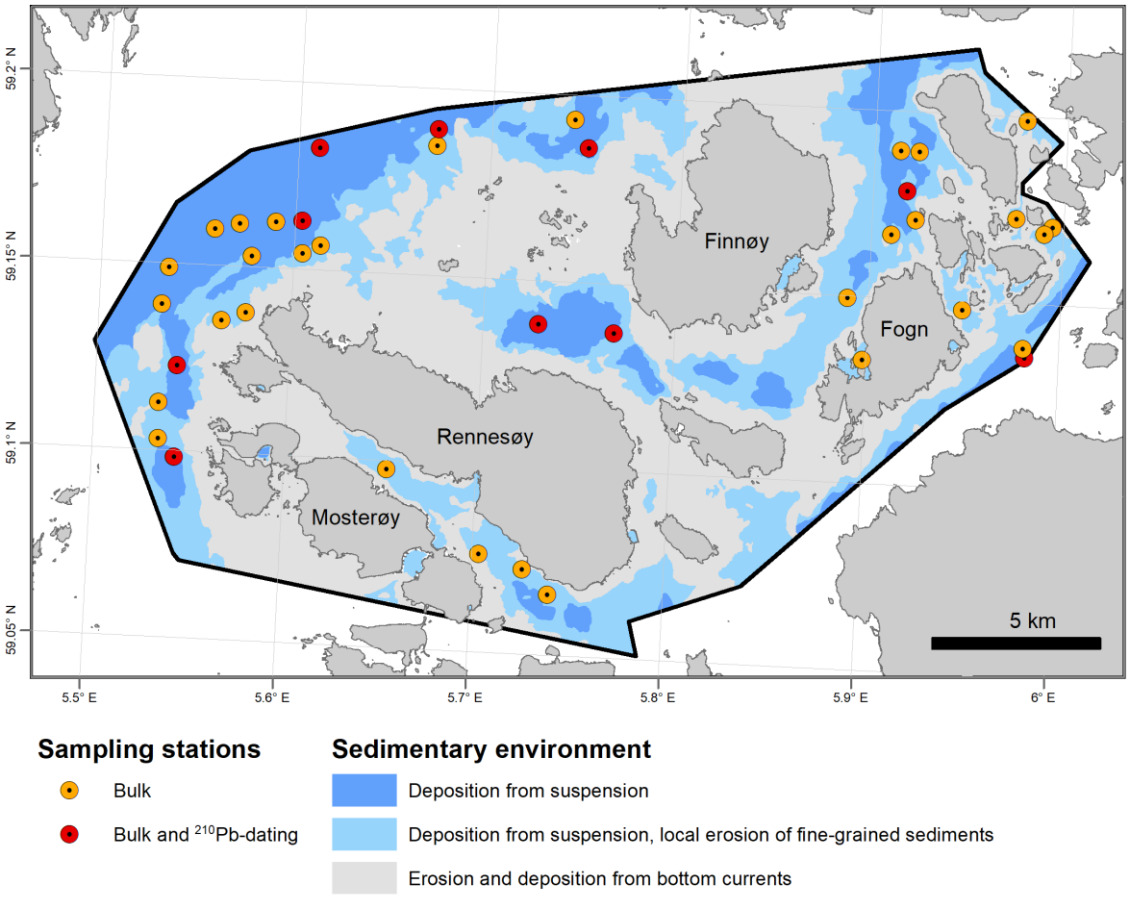


**Figure 2. Overview of sampling stations. Bulk samples of the upper 10 cm of the sediment were collected at 40 stations. Multi cores for $^{210}$Pb-dating were collected at a subset of the bulk sampling stations.**

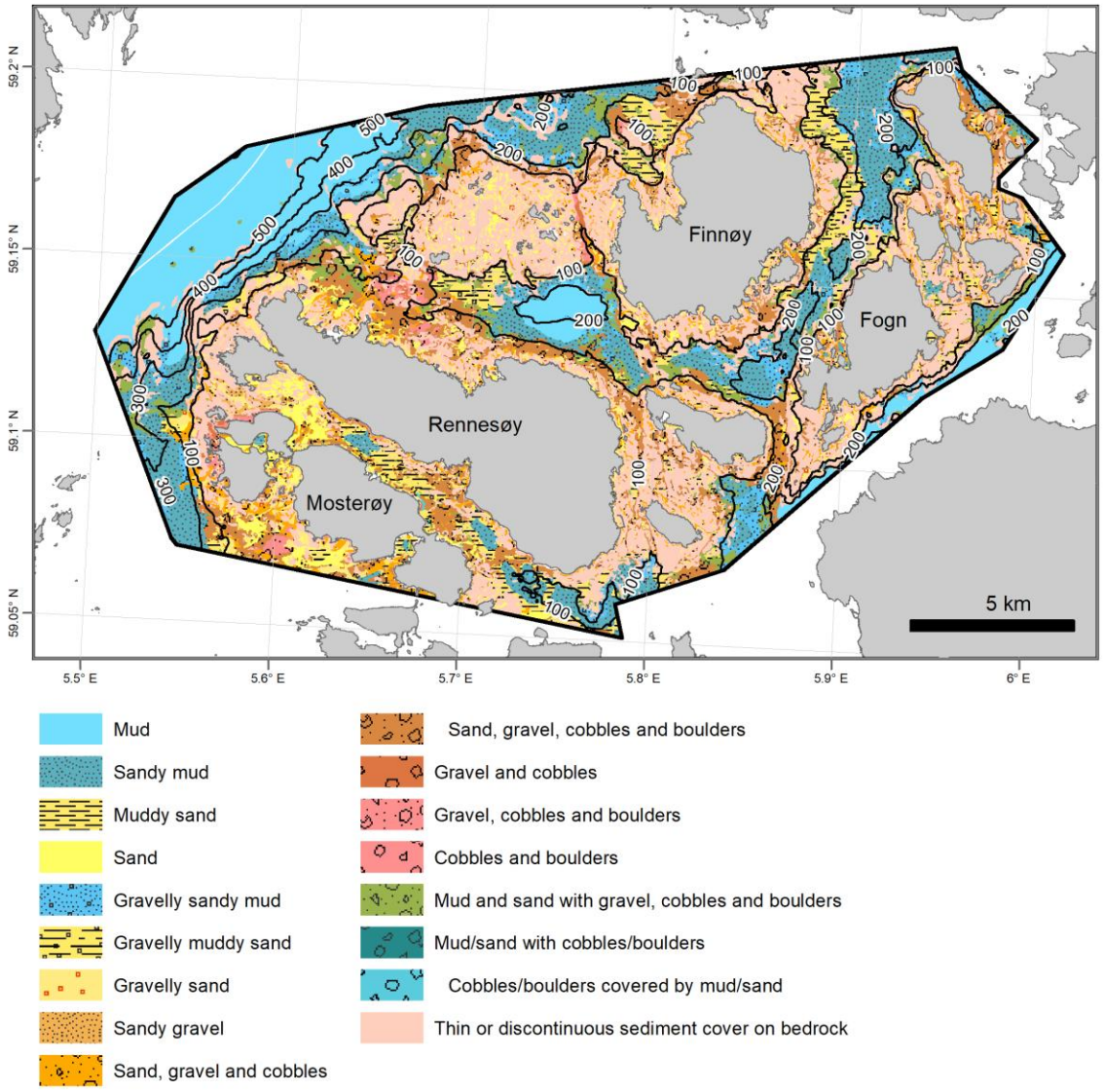


**Figure 3. Substrate types in the core study site. Isobaths are shown in 100 m-intervals.**

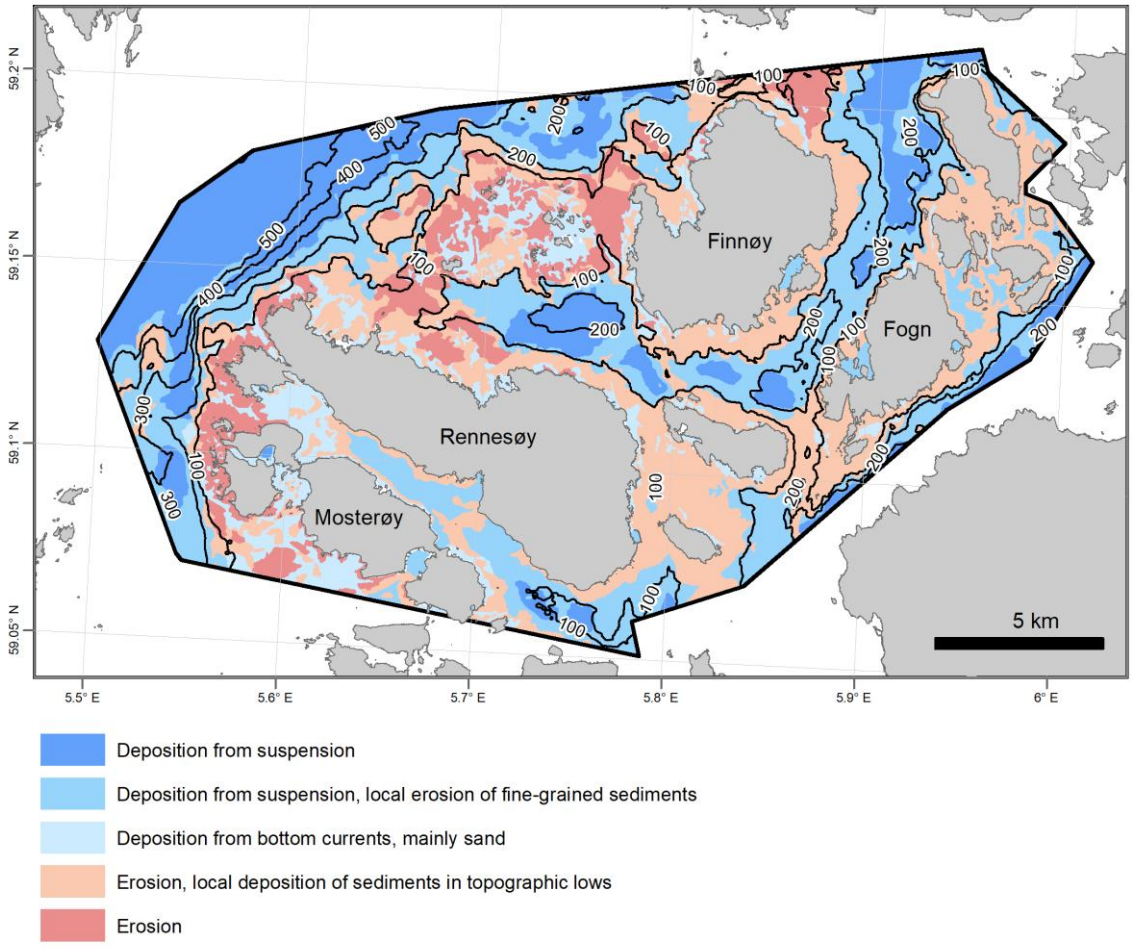


650

**Figure 4. Sedimentary environment in the core study site. Isobaths are shown in 100 m-intervals.**

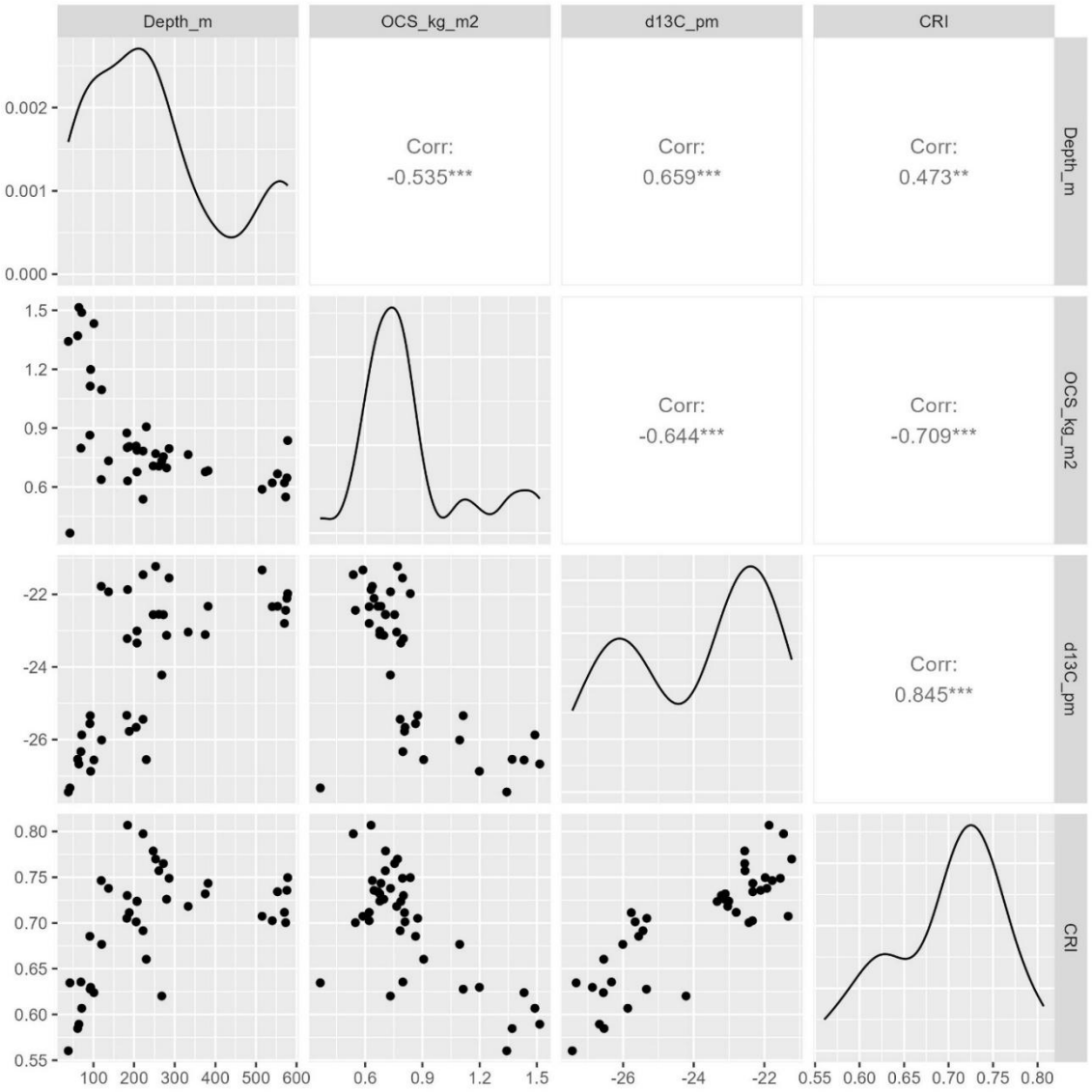


**Figure 5. Generalised pairs plot showing the relationships between the response variables and water depth. Corr: Pearson product moment correlation coefficient. Asterisks indicate p-values. **: $p < 0.01$ and ***: $p < 0.001$.**

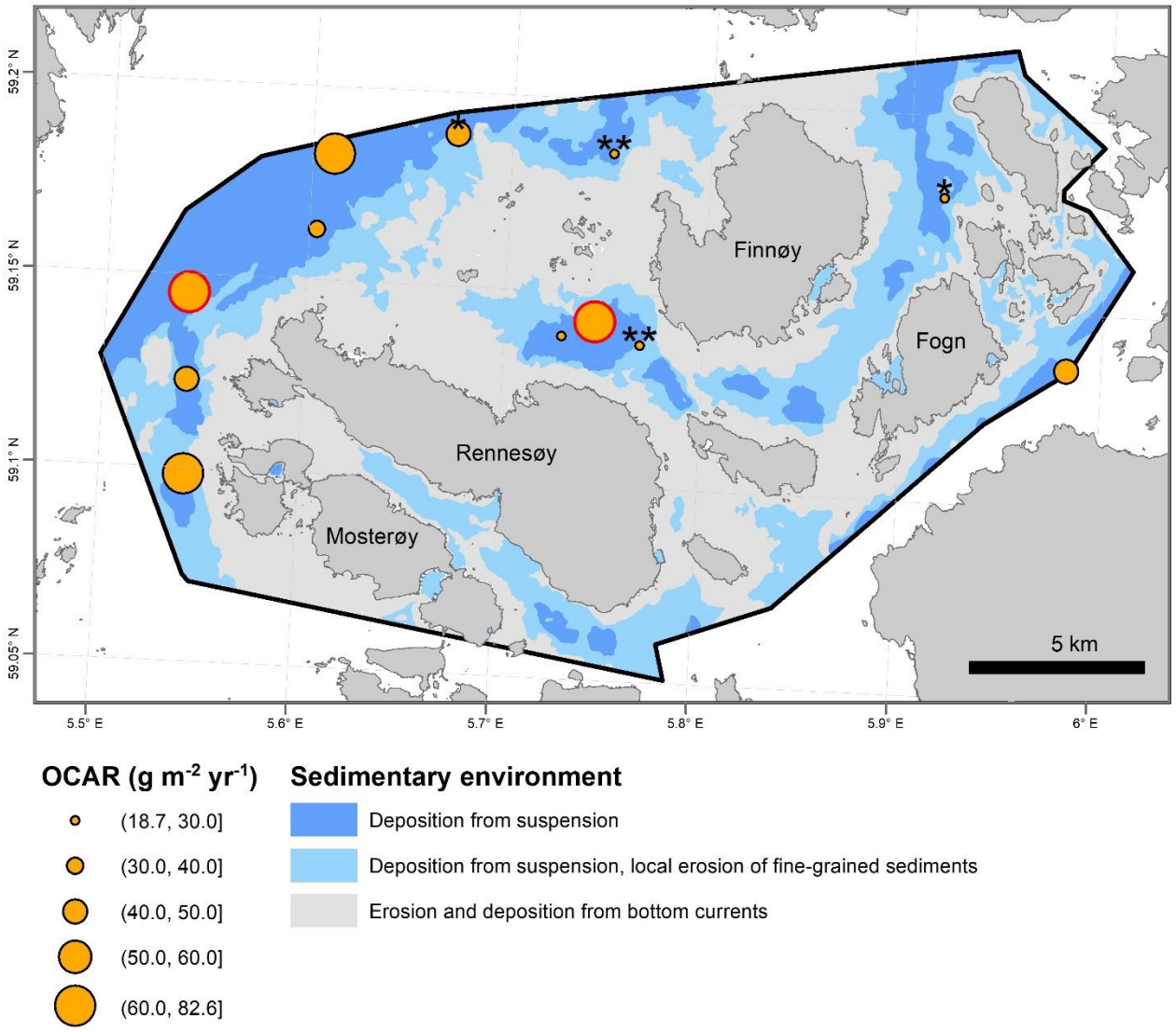


**Figure 6. Organic carbon accumulation rates ($OCAR_{10}$). Cores were collected within areas mapped as deposition from suspension (see Figure 4). One asterisk (*) indicates cores potentially affected by sediment mixing and two asterisks (**) indicate cores affected by sediment mixing. Circles with red outline indicate cores taken by Knies et al. (2021a).**

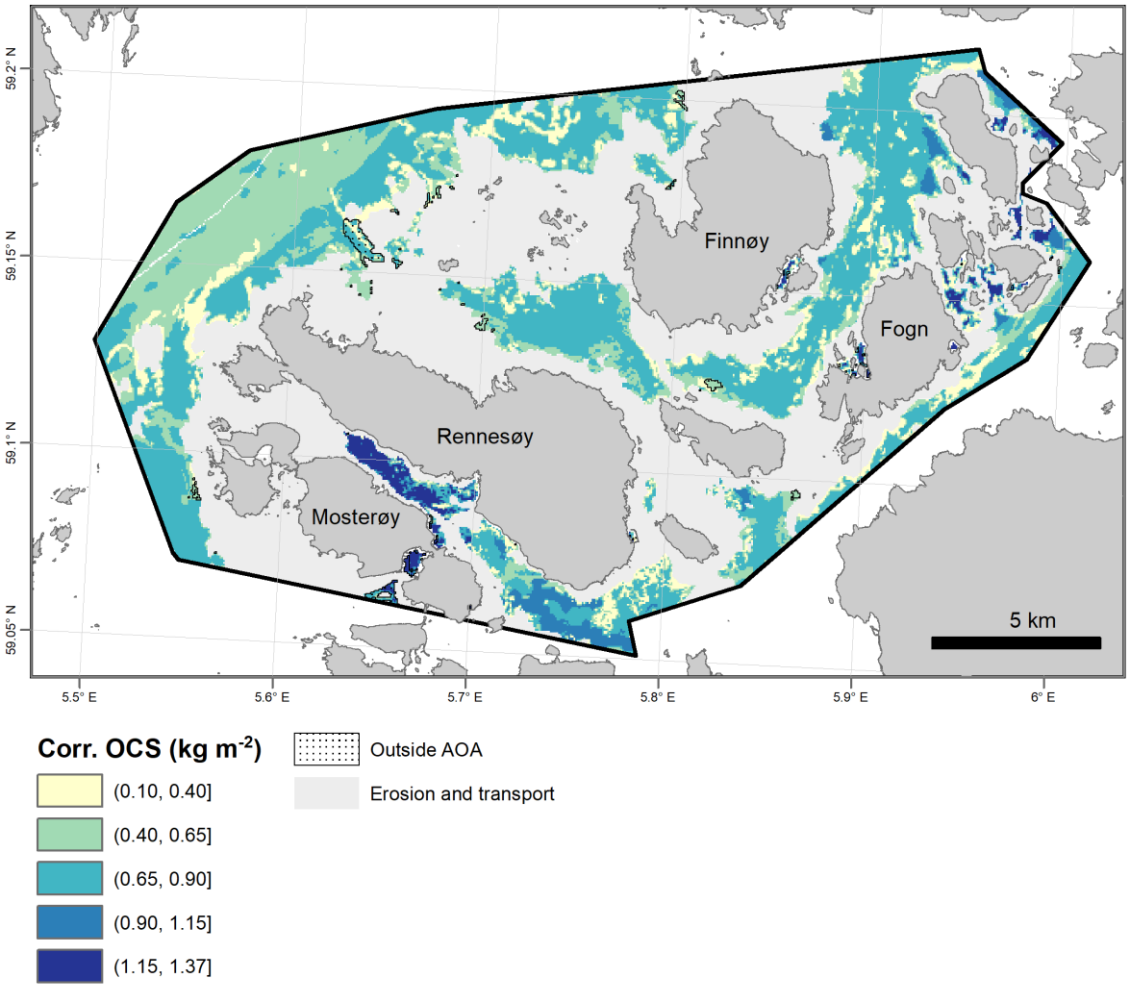


**Figure 7. Corrected organic carbon stocks (OCS) of the upper 10 cm of the sediment. Predictions outside the area of applicability (AOA) of the model are shown as well.**

665

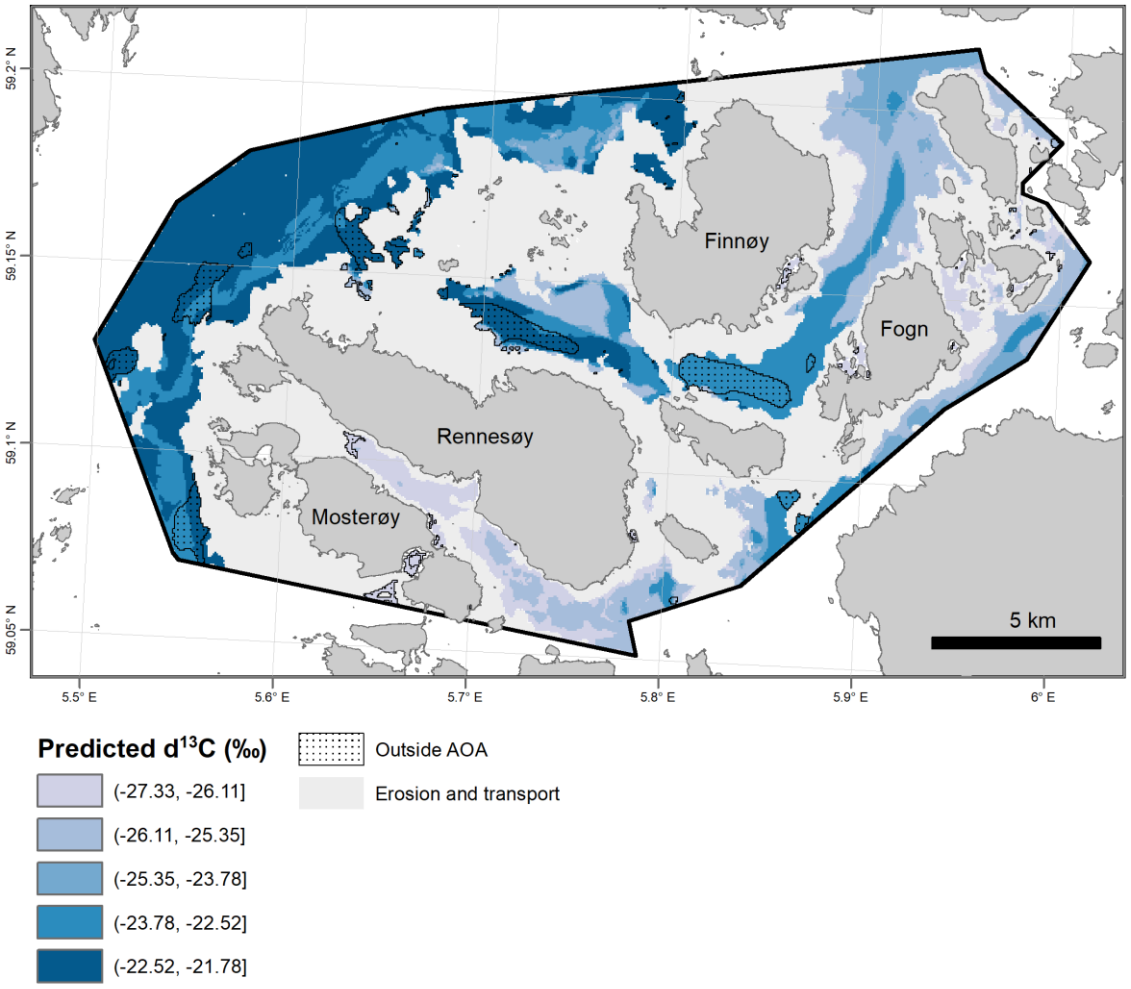


**Figure 8. Stable carbon isotope ($\delta^{13}C$) values. Predictions outside the area of applicability (AOA) of the model are shown as well.**

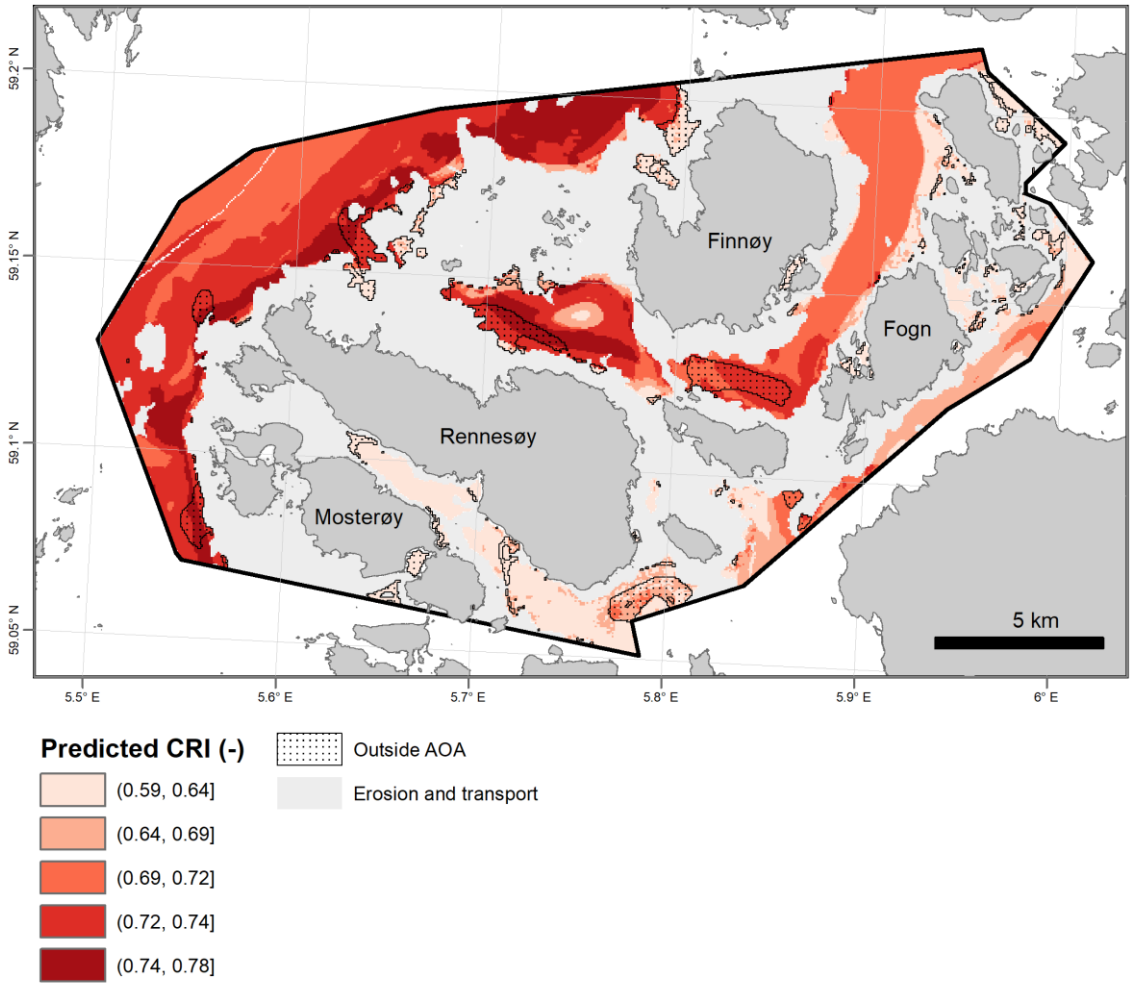


670 **Figure 9. Carbon reactivity index (CRI). Predictions outside the area of applicability of the model are shown as well.**

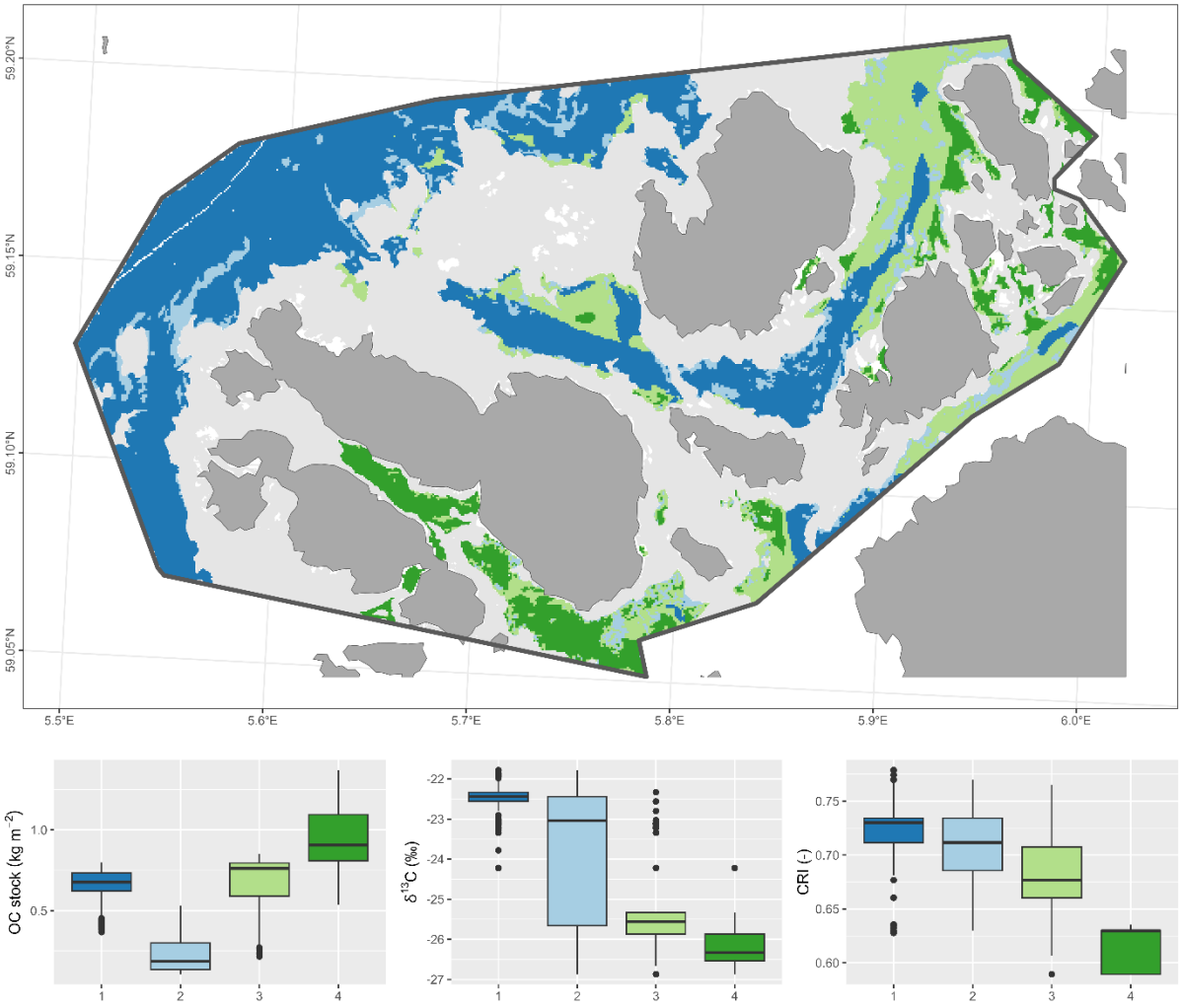


**Figure 10. Regionalisation with four clusters. Boxplots of the variables used for clustering show the properties of the clusters. The thick horizontal line of the boxplots is the median, the ends of the box are the upper (Q3) and lower (Q1) quartiles, defining the interquartile range (IQR), the whiskers show the range of values within Q3 + 1.5 × IQR to Q1 - 1.5 × IQR, representing the highest and lowest values, excluding outliers and outliers are the dots beyond the whiskers.**